Numerical Investigation on Trapezoidal Cavity Receiver Used In LFR with Water Flow in Absorber Tubes

Rohit Duggal[1, *] **and Ravindra Jilte**[2]

[1] Research Scholar, School of Mechanical Engineering, Lovely Professional University, Jalandhar, Punjab 144411, India
[2] Professor, School of Mechanical Engineering, Lovely Professional University, Jalandhar, Punjab 144411, India

[*]Corresponding author: rohitduggal195@gmail.com

Abstract. In the present study, numerical three dimensional model of trapezoidal cavity used in LFR was analysed. Results are presented in the form of Thermal losses occurring from the receiver operating with an absorber tube temperature from 350-550 K in step of 50 K and emissivity varied from 0.5-1.0. Effect of wind blowing below lower glass plate (cavity aperture) were also analysed considering the heat transfer coefficient from 5 to 25 W/m^{2}K. At lower absorber temperature (350 K) convective losses is found to be 43% of the total heat loss whereas radiative losses accounted 57%. For higher absorber temperature radiative losses are dominant (77%) and convective losses are reduced to 23%. The air temperature gradient in the horizontal direction (parallel to lower glass plate) is found to be negligible whereas it is varied significantly in vertical direction (normal to lower glass plate). The average cavity air temperature is observed to be 480 K for low wind flow (h=5 W/m^{2}K) and it reduces to 360 K for h=25 W/m^{2}K. This has resulted in increased convective losses (27% higher).

1. Introduction

Among the various types of Concentrating Solar Power (CSP) plants, Linear Fresnel Reflector (LFR) technology is considered prospective due to low cost and structural simplicity. Moreover, merits related to cost associated with manufacturing, operation and maintenance is less as compared to Parabolic Trough Collector (PTC) [1-3]. The advantages associated with Fresnel Lens mainly small volume, light weight, low cost mass production and increasing the energy density has paved the way for its application in solar thermal field [4]. An LFR CSP consists of three main components: concentrator, receiver and absorber. It consists of linear array of mirrors that concentrate solar radiation on to a downward facing receiver containing pipe absorbers. These pipes contain a particular Heat Transfer Fluid (HTF) which absorbs energy and applies to power generation. Generally, receiver in the form of inverted trapezoidal shape is preferred [5] (insulated upper and side surfaces, absorber tubes with steam beneath top face and lower glass plate to allow solar flux onto absorber tubes). The performance of the LFR is affected by the thermal losses in the receivers (both radiative and convective) occurring from high temperature absorber tube. Several studies have been attempted to study the heat transfer from the LFR receiver. Pye et al. [6] have studied unsteady flow patterns in trapezoidal cavity receiver. Unsteadiness in the flow structure do not significantly vary overall heat transfer losses. Reynolds et al. [5] analyzed the heat losses from the absorber of trapezoidal receiver. 8% higher efficiency was obtained with round pipes as compared to rectangular absorber pipes. Further,

Singh et al. [7] investigated that thermal efficiency is influenced by surface coating and concentration ratio. The thermal efficiency correlations were developed for absorber surface coating as a function of concentration ratio and entry HTF temperature. Furthermore, deviation in correlated and experimental data was reported for rectangular and round absorber pipe. In addition, Singh et al. [8] investigated heat transfer coefficient for single and double glass cover as well as absorber surface coating. It was concluded that heat losses in nickel black coating was 30% less as compared to matt black absorber coating. Moreover, in case of single glass cover, varying the absorber temperature reduces heat losses for round tubes unlike double layer glass cover where difference in heat losses for both (round and rectangular) absorbers is negligible. Further, the correlations between overall heat transfer coefficient and absorber surface temperature were presented and reported that experimental and correlated data agree to great extent. Facao and Oliveira [9] divided the pipes into two halves and cavity was modelled. The numerical study was carried out considering surface radiation, cavity convection and wall conduction thereby observing least global heat loss coefficient for 45mm cavity depth. Reddy et al. [10] investigated heat transfer and presented Nusselt number correlations for different parameters of trapezoidal cavity receiver considering isothermal top and bottom glass cover. The side walls of cavity were modelled with 0.5 W/m2K as heat loss coefficient and 0.3 as internal emissivity, however, bottom heat loss due to forced convection leading from blowing wind was neglected. Sahoo et al. [11] numerically investigated the thermal losses in trapezoidal cavity with eight absorber tubes. Inside the cavity, isotherms and flow patterns were analyzed ensuring the gaps between absorber tubes and non-dimensionalization was adopted for reporting the results. This study reported different correlations for Nusselt number excluding radiation and conduction parameter. Further Sahoo et al. [12] applied the heat transfer model to investigate the methodology of multiphase flow in absorber tubes. The variation in parameters for single phase region (bulk fluid temperature, pressure drop and heat transfer coefficient) and for two phase region (dryness fraction, pressure loss and local boiling point) was presented. Moghimi et al. [2] carried out computational study to optimize the cavity for lesser heat transfer losses. The LFR cavity was modelled considering four round pipes and walls were assumed as insulated. The fluid inside the cavity was considered as incompressible and density was chosen as a function of temperature. Discrete Ordinate Method was chosen to simulate radiation heat loss and optimized for lesser side wind loss.

Based on the aforementioned studies, it was observed that in numerical investigations actual HTF flow inside the absorber tubes were not considered. The present study focuses on three dimensional numerical investigations on trapezoidal cavity receiver considering both airside as well as HTF side heat losses. However, only the airside results are included in the present paper.

2. Receiver description

A symmetric schematic sketch of cavity located at focal point of LFR system is shown in figure 1. The Heat Transfer Fluid (HTF) is taken as water and air is taken inside the cavity. A closed three-dimensional trapezoidal receiver cavity is considered containing eight tubes having a small gap in between allowing thermal expansion. The tubes are of Nominal Pipe Size (NPS) 1 stainless steel (SS) 304 material configuration. There is a glass covering at bottom of receiver cavity to allow solar radiations inside the cavity. The outer covering of other three sides is insulated to minimize the heat losses. The reflected rays from linear array of mirrors arranged at the bottom falls on the absorber tubes thereby increasing the temperature of HTF flowing.

3. Numerical analysis

3.1. Model description

In the present study, three-dimensional model is adopted to predict the heat loss from the receiver cavity. For the purpose of generating mesh as shown in figure 2, the Meshing package of ANSYS 15 Workbench is used. The accuracy and convergence of the solution for the computational domain is checked for skewness and aspect ratio, which should not exceed certain value (0.85) as reported by

Bakker [13]. The maximum and minimum values of skewness (max. 0.68 and min. 0.032) and aspect ratio (max. 5.86 and min. 1.10) for present study with the average element quality as 0.811 provides the quality mesh for computational domain.

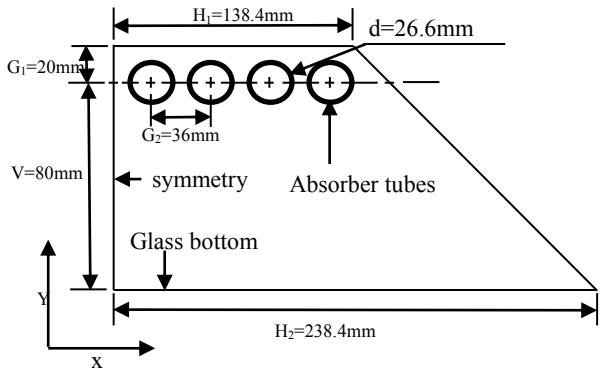

Figure 1. Sketch of receiver cavity.

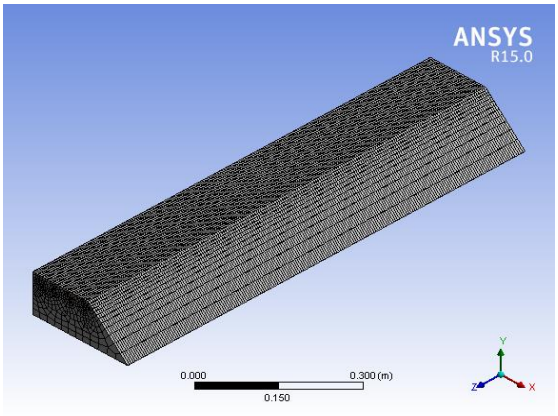

Figure 2. Receiver cavity mesh.

The values obtained from numerical simulations are a result of simultaneous solution of the system of flow and heat transfer equations describing mass, momentum, energy. The equations can be described as below [14]:

Continuity equation

$$\frac{\partial(\rho u)}{\partial x}+\frac{\partial(\rho v)}{\partial x}=0 \tag{1}$$

Momentum equation

$$\left(u\frac{\partial u}{\partial x}+v\frac{\partial u}{\partial y}\right)=-\frac{1}{\rho}\frac{\partial P}{\partial x}+\vartheta\left(\frac{\partial^2 u}{\partial x^2}+\frac{\partial^2 u}{\partial y^2}\right)+g\beta(T-T_h) \tag{2}$$

Energy equation

$$\left(u\frac{\partial T}{\partial x}+v\frac{\partial T}{\partial y}\right)=\alpha\left(\frac{\partial^2 T}{\partial x^2}+\frac{\partial^2 T}{\partial y^2}\right) \tag{3}$$

The current work has 350-550 K of temperature range therefore the Boussinesq approximation is invalid. Since, in this temperature range, the product of temperature difference between wall surface and air with the coefficient of thermal expansion of air (0.142-0.58) is higher than 0.1 for Boussinesq approximation to be applied [15]. Hence non-Boussinesq approximation, i.e. the ideal gas characteristics are chosen for cavity air and above equation is used to solve steady, laminar natural convection model. The surface to surface (S2S) radiation model is coupled with natural convection model. S2S model assumes that the working fluid is not participated in absorption, emission and scattering of radiation. The main assumption of S2S radiation model is that the surfaces are grey and diffuse. However, it should be noted that model assumes heat transfer is affected between two surfaces depending upon their size, orientation and separation distance. View factors are used to account the influence of these variables [16].

3.2. Boundary conditions

Different boundary conditions are applied to the cavity receiver. No slip conditions are assumed at walls. Fluids are taken to be incompressible and Newtonian. Since, tubes are continuously subjected to solar radiations therefore tubes are assumed to be at uniform constant temperature after reaching stagnation conditions. Therefore, isothermal boundary conditions are chosen for absorber tubes. The outer covering of cavity receiver is insulated so as to reduce heat losses. Thus, adiabatic conditions are assumed for outer covering. There is radiative heat loss among the walls of receiver cavity due to the high temperature. Moreover, convection losses are significant with bottom glass cover to surrounding air. Hence, both convection and radiation boundary conditions are applied to glass covering. Mainly,

top wall, side wall, bottom wall and absorber tube emissivity as 0.1, 0.1, 0.9 and 0.49-0.9 respectively. External emissivity of bottom wall and heat transfer coefficient as 0.9 and 5.0-25.0 W/m^{2}K. Temperature of absorber tube is varied from 350-550K.

3.3. Numerical procedure

The simulation for turbulent incompressible flow are carried out using FLUENT 15 software package. The standard (k-Ɛ) 2-eq model is chosen to model turbulent conditions, since it is most widely used engineering model which includes sub-model for buoyancy [16]. Second order upwind scheme is used for discretization of pressure velocity coupling equations. For residuals of continuity and momentum equations, a convergence criterion of 10^{-3} was imposed whereas 10^{-6} as energy equation residuals. The convergence is determined by the residual levels and also by monitoring relevant integrated quantity like heat transfer coefficient. The solutions are obtained only after satisfying convergence criterion.

3.4. Grid independence study

To lower the dependency of grid on the obtained solutions different grids were studied. Since, greater the number of elements, lesser is the deviation in solution. Therefore, different number of elements is chosen for the grid to check the solution dependency with respect to the grid. The geometry is divided into quadrilateral and hexahedral unstructured mesh elements ranging from 71,050 to 3,35,274. Table 1 below shows the variation of total heat transfer with respect to the grid size. It is further seen that the variation in heat transfer solution for elements 71,050 and 1,11,600 is negligible (<1%). Hence, 71,050 elements are sufficient to model the geometry to obtain reliable results. Thereby, reducing the computational time and cost on a greater extent.

3.5. Validation and verification of numerical procedure

In order to validate computational results, the simulation values obtained for total heat loss are compared with experimental data obtained by Sahoo et. al. [12] using their cavity lab test setup. It can be seen from figure 3, that the results obtained from simulated data are well in conformation with experimental data.

Table 1. Cavity grid independence study.

Number of elements	Total heat loss (W)	% change in heat loss
71050	106.822	
111600	106.828	0.06
268128	107.830	0.93
335274	107.409	-0.39

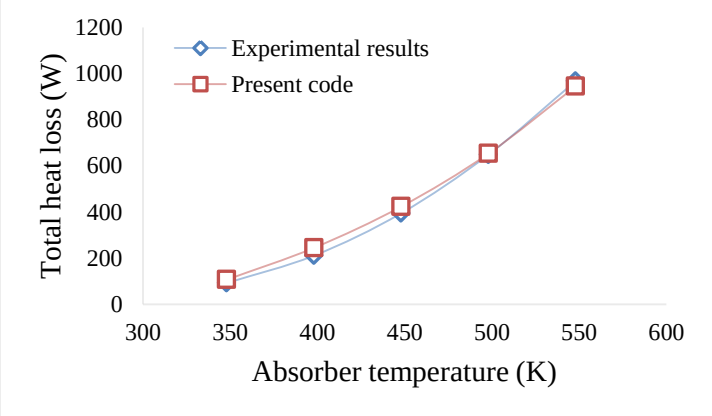

Figure 3. Comparison of Total heat loss (W) with Sahoo et. al. [12] and present numerical simulation.

4. Results

4.1. Isotherm contours

Isotherms contours are plotted in figure 4 and 5 for various cavity parameters. It can be seen from isotherm contours in figure 4 that temperature variations along horizontal direction is almost negligible and hence uniform profile is seen. However, natural convection is taking place due to the

temperature gradient along vertical direction. Thus, rising the air from centre of cavity and settling down from the side surfaces. Further, as the absorber tube temperature is increased the heat affected zone with higher average temperature shifts towards bottom glass cover thereby increasing the vertical temperature gradient. figure 4 (a) shows the approximate average temperature 375.5 K which increases as absorber temperature increases up to 487.5 K. However, the percentage vertical temperature gradient is reduced from 9.09% to 7.14% as temperature varies from 350 K to 550 K respectively this is due to the increased losses at higher temperatures.

It can be observed from figure 5 that as the heat transfer coefficient near glass surface is increased there are significant convective losses. The amount of cooling of air that is taking place near the glass surface as a result of ambient air conditions can be observed easily by varying the heat transfer coefficient. It can be seen that for h=5 W/m^{2}K almost all the entrapped air (90% approx.) is at higher average temperature (480 K approx.). However, the amount of entrapped air with higher temperature is reduced from 90% to approximately 40% with increased value of heat transfer coefficient (h=5 to 25 W/m^{2}K). The average temperature is also reduced from 480 K to 360 K as the value of heat transfer coefficient is increased (h=5 to 25W/m^{2}K). It can be concluded from above results that with lesser value of average temperature more heat is being swept away due to blowing wind. Thus, ambient environment conditions significantly affect the heat loss characteristics of the cavity.

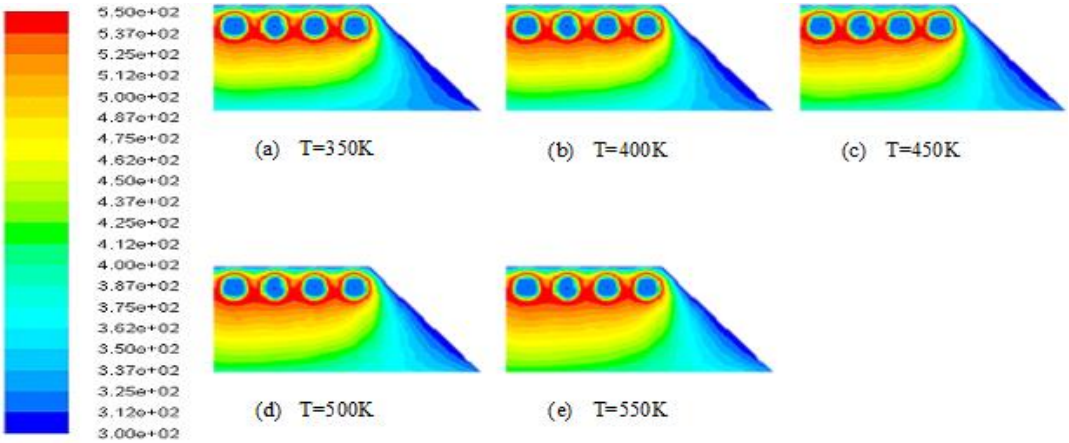

Figure 4. Cavity isotherm contours for m=0.1kg/s, h=5W/m^{2}K, Ɛ=0.49 at different absorber temperatures.

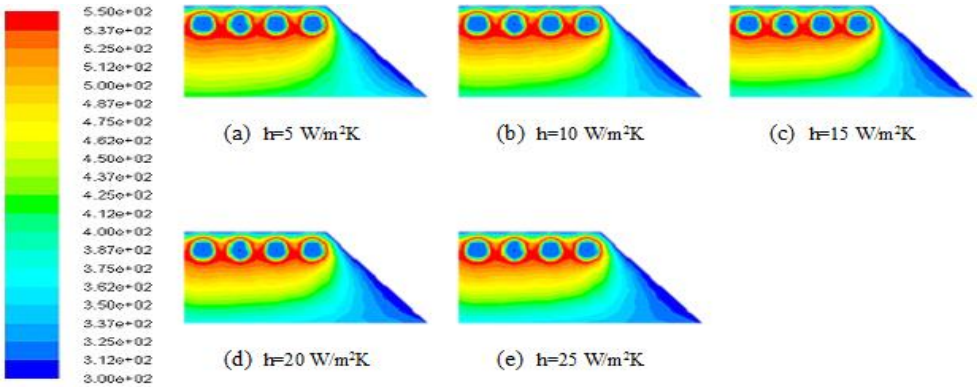

Figure 5. Cavity isotherm contours for m=0.1kg/s, Ɛ=0.49, T=550K at different heat transfer coefficient.

4.2. Cavity heat exchange

4.2.1. Effect of absorber temperature on heat loss characteristics. Figure 6 shows the variation of heat transfer taking place inside the cavity as a function of absorber surface temperature. It is observed that as the wall temperature of absorber tubes increase heat loss is increased for m=0.1kg/s, h=5W/m^{2}K and Ɛ=0.49. Radiative heat loss for temperature 400 K is 244.57 W and for temperature 450 K is 423.32 W showing 87.21% increase in value. The percentage change is decreased from 87.21% to 52.33% as the absorber temperature is increased to 550 K. The convective heat loss amounts to 90.57 W for 400 K and 135 W for 450 K absorber temperature. Thus, there is an increase of 49% in convective losses. This percentage increase changes from 49% to 24.3% as temperature reaches to 550 K. Thus, it is clear that radiative heat losses steep more as compared to convective losses. This is due to the higher temperature of absorber tubes emitting radiation and contributing to radiation losses. It is further observed that at higher absorber temperature (550 K) radiative heat losses are dominant, i.e. 76.45% of the total heat loss for the receiver cavity.

4.2.2. Effect of Rayleigh number. The variation of Nusselt number with respect to Rayleigh number can be observed in figure 7. It is clearly obtained from the graph that Nusselt number is an increasing function of Rayleigh number. As Rayleigh number is increased so does the Nusselt number.

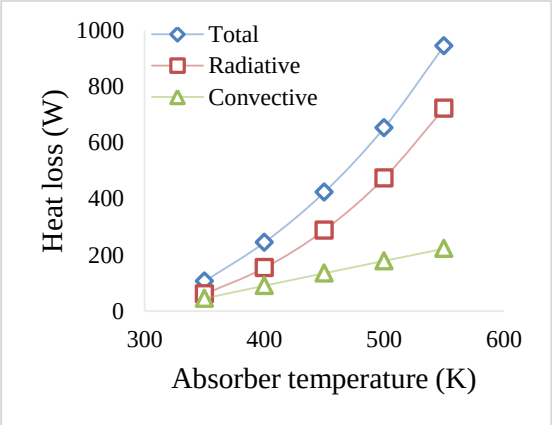

Figure 6. Heat loss characteristics (total, radiative and convective) for m=0.1kg/s, h=5W/m^{2}K and Ɛ=0.49.

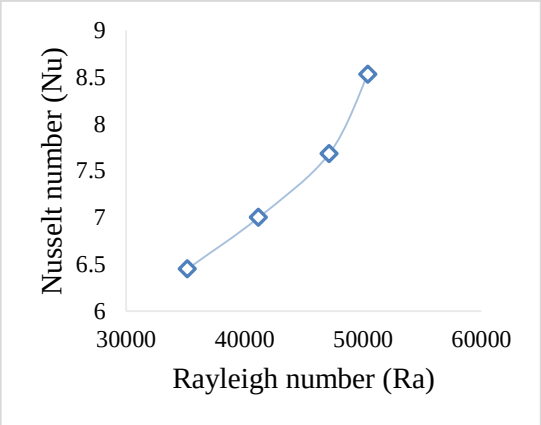

Figure 7. Variation of Nusselt number (Nu) for m=0.1kg/s, h=5W/m^{2}K, Ɛ=0.49.

4.2.3. Effect of absorber emissivity. The heat loss characteristics as a function of absorber tube emissivity can be obtained from figure 8. It is observed that convective heat losses are more or less uniform as well as negligible. The radiation losses are dominant as the emissivity values are varied. Radiative heat exchange is increased with increasing values of absorber tube emissivity.

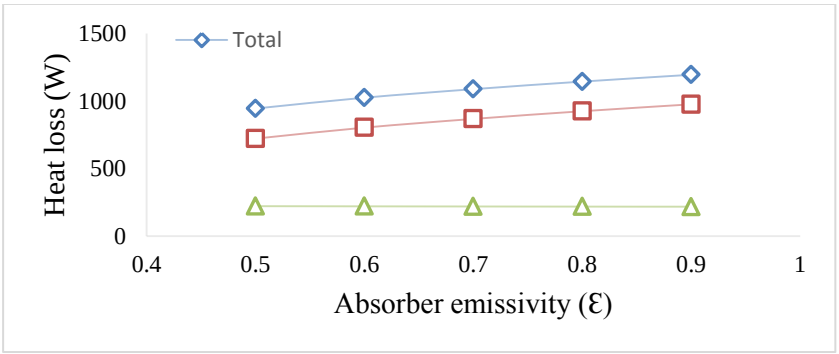

Figure 8. Heat loss characteristics (total, radiative and convective) for m=0.1kg/s, h=5W/m^{2}K, T=550.

5. Conclusions

In the present study, numerical three dimensional model of trapezoidal cavity used in LFR was analysed considering actual HTF flow in absorber tubes. Relative dominance of convective and radiative losses was evaluated. At lower absorber temperature (350 K) convective losses is found to be 43% of the total heat loss whereas radiative losses accounted 57%. For higher absorber temperature (550 K) radiative losses are dominant (77%) and convective losses are reduced to 23%. The cavity air temperature is used to calculate air temperature gradient for studying the effect of wind blow on lower glass plate as well as varied absorber tube temperatures. The air temperature gradient in the horizontal direction (parallel to lower glass plate) is found to be negligible whereas it is varied significantly in vertical direction (normal to lower glass plate). The average cavity air temperature is observed to be 480 K for low wind flow (h=5 W/m^2K) and it reduces to 360 K for h=25 W/m^2K. This has resulted in increased convective losses (27% higher).

6. References

[1] Mills, D.R., Morrison, G.L., 2000. Compact linear fresnel reflector solar thermal power plant. Sol. Energy 68, 263–283.
[2] Moghimi, M.A., Craig, K.J., Meyer, J.P., 2015. Optimization of a trapezoidal cavity absorber for the linear Fresnel reflector. Sol. Energy 119, 343–361.
[3] El Gharbia N, Derbalb H, Bouaichaouia S, Saida N. A comparative study between parabolic trough collector and Linear Fresnel Reflector technologies. Energy Proc 2011;6:565–72.
[4] Xie, W.T., Dai, Y.J., Wang, R.Z., 2011a. Numerical and experimental analysis of a point focus solar collector using high concentration imaging PMMA Fresnel lens. Energy Conversion and Management 52 (6), 2417–2426.
[5] Reynolds, D.J., Jance, M.J., Behnia, M., Morrison, G.L., 2004. An experimental and computational study of the heat loss characteristics of a trapezoidal cavity absorber. Sol. Energy 76, 229–234.
[6] Pye, J.D., Morrison, G., Behnia, M., 2003a. Transient modeling of cavity receiver heat transfer for the compact linear Fresnel reflector. In: ANZESES Destination Renewable 69-77.
[7] Singh, P.L., Sarviya, R.M., Bhagoria, J.L., 2010a. Thermal performance of linear Fresnel reflecting solar concentrator. Appl. Energy 87, 541–550.
[8] Singh, P.L., Sarviya, R.M., Bhagoria, J.L., 2010b. Heat loss study of trapezoidal cavity absorbers for linear solar concentrating collector. Energy Convers. Manage. 51, 329–337.
[9] Facao, J., Oliveira, A.C., 2011. Numerical simulation of trapezoidal cavity receiver for a linear Fresnel solar collector concentrator. Renew. Energy 36, 90–96.
[10] Reddy, K.S., Natarajan, S.K., Mallick, T.K., 2012. Heat losses characteristics of trapezoidal cavity for solar linear concentrating system. Appl. Energy 93, 523–531.
[11] Sahoo, S.S., Singh, S., Banerjee, R., 2012. Analysis of heat losses from a trapezoidal cavity used for linear Fresnel reflector system. Sol. Energy 86, 1313–1322.
[12] Sahoo, S.S., Singh, S., Banerjee, R., 2013. Steady state hydrothermal analysis of the absorber tubes used in linear Fresnel reflector solar thermal system. Sol. Energy 87, 84–95.
[13] Bakker, A., 2013. Lecture 7 – Meshing, Applied Computational Fluid Dynamics
[14] Jiji, J. L. M. (2006). *Heat Convection*. Springer-Verlag
[15] Gray, D. D., & Giorgini, A. (1976). The validity of the Boussinesq approximation for liquids and gases. International Journal of Heat and Mass Transfer, 19, 545-551
[16] ANSYS, 2013b. Design Exploration User Guide, version 15, ANSYS Incorporated